

## Crystallization of the collagen-like polypeptide (PPG)<sub>10</sub> aboard the International Space Station.

### 1. Video observation

Alessandro Vergara,<sup>a</sup> Ermanno Corvino,<sup>a</sup> Giosué Sorrentino,<sup>b</sup> Chiara Piccolo,<sup>c</sup> Alessandra Tortora,<sup>c</sup> Luigi Carotenuto,<sup>c</sup> Lelio Mazzarella<sup>a</sup> and Adriana Zagari<sup>d\*</sup>

<sup>a</sup>Dipartimento di Chimica, Università degli Studi di Napoli, Italy, <sup>b</sup>CNR, Istituto di Biostrutture e Bioimmagini, Napoli, Italy, <sup>c</sup>MARS Center, Napoli, Italy, and <sup>d</sup>Dipartimento di Chimica Biologica, Università degli Studi di Napoli, Via Mezzocannone 6, Napoli, Italy. E-mail: zagari@chemistry.unina.it

Single chains of the collagen model polypeptide with sequence (Pro-Pro-Gly)<sub>10</sub>, hereafter referred to as (PPG)<sub>10</sub>, aggregate to form rod-shaped triple helices. Crystals of (PPG)<sub>10</sub> were grown in the Advanced Protein Crystallization Facility (APCF) both onboard the International Space Station (ISS) and on Earth. The experiments allow the direct comparison of four different crystallization environments for the first time: solution in microgravity ( $\mu$ g), agarose gel in  $\mu$ g, solution on earth, and gel on earth. Both on board and on ground, the crystal growth was monitored by a CCD video camera. The image analysis provided information on the spatial distribution of the crystals, their movement and their growth rate. The analysis of the distribution of crystals reveals that the crystallization process occurs as it does in batch conditions. Slow motions have been observed onboard the ISS. Different to Space-Shuttle experiment, the crystals onboard the ISS moved coherently and followed parallel trajectories. Growth rate and induction time are very similar both in gel and in solution, suggesting that the crystal growth rate is controlled by the kinetics at the interface under the used experimental conditions. These results provide the first data in the crystallogenesis of (PPG)<sub>10</sub>, which is a representative member of non-globular, rod-like proteins.

**Keywords:** crystallogenesis, advanced protein crystallization facility, microgravity.

### 1. Introduction

The quality of the crystals is a major issue in protein crystallography. The ability to obtain good quality crystals is a mandatory requirement of any crystallographic study to determine high-resolution protein structures (Giegé & McPherson, 2001). Consequently, many suggestions were given to crystal growers, to allow the resolution of a continuously raising number of structures. New crystallization techniques and new crystallization environments were suggested to get improved crystals for X-ray analysis. The Genomic program strongly contributed to raise the interest of the scientific community in this field.

The reduced gravity environment was tested as a possible way to achieve a better quality of protein crystals, because in these conditions, possible defects due to sedimentation and convection are expected to be depleted (McPherson, 1996). The validity of this environment to grow crystals was much argued in the past (Couzin, 1998; Chayen & Helliwell, 1999) and it is still a current topic in biotechnology (DeLucas, 2001). This paper provides new results to this debate.

### 1.1. Scientific background

Several space missions were devoted to monitor the crystal growth process, *via* video and interferometric observations by using the Advanced Protein Crystallization Facility (APCF) (Bosch *et al.*, 1992). Hereafter we briefly review some interesting analyses of video observations in some space missions to which will be referred throughout the present work. During the space mission STS-65, Chayen *et al.* (1997) monitored with a CCD camera both a halo effect, attributed qualitatively to the depletion zone around crystals, and a crystal motion ascribed to the Marangoni convection present in hanging drop experiments. García-Ruiz & Otalora (1997) gave a detailed description of the procedure to analyse images recorded by video observation, as well as observing crystal motion in a number of other space-missions. Snell *et al.* (1997) analysed the correlation between fluctuation in the growth rate and data of the accelerometer during the IML-2 mission. Lorber *et al.* (1999) analysed the number, size and growth rate both in microgravity ( $\mu$ g) and on ground, during the USML-2 and LMS missions.

The absence of convection and sedimentation is the major advantage expected when crystallizing macromolecules in  $\mu$ g. However, the residual acceleration and the resulting crystal motion are considered as drawbacks of the otherwise successful experiments. For this reason some space missions were devoted to the crystallization in gel (Miller *et al.*, 1992; De Lucas *et al.*, 1994; Dong *et al.*, 1999; Otalora *et al.*, 2001; Zhu *et al.*, 2001). In fact, the use of gel could be a remedy, because crystals are almost immobilized. The history of crystallization of conventional solutes in gel is a century old (Henisch, 1988 and therein); nevertheless, the first attempts to use gel in protein crystallization were cited in Robert & Lefaucheur (1988), followed by several experimental set-ups, as gel acupuncture (García-Ruiz *et al.*, 1993). Agarose gel was well characterized; indeed its structural (Pernodet, *et al.* 1997; Maaloum, *et al.* 1998; Kouwijzer & Perez, 1998), mechanical (Normand *et al.*, 2000; García-Ruiz *et al.* 2001a) and transport properties information (Muhr & Blanshard, 1982; Johnson *et al.*, 1996; Kong *et al.*, 1997; Amsden, 1998; Stigter, 2000) is available in literature. Hereafter, we schematically summarise the space missions devoted to compare the crystallization process in solution and gel,  $\mu$ g and earth. We will refer to experiments in APCF performed by the group of Giegé (Lorber *et al.*, 1999), Helliwell (Dong *et al.*, 1999), Garcia-Ruiz (Otalora *et al.*, 2001) along with others in different facilities by Carter (Miller & Carter, 1992) and DeLucas (De Lucas *et al.*, 1994). Scientific reasons motivate the use of different environments in previous missions: Lorber *et al.* (1999) compared the quality of crystals grown in gel, in  $\mu$ g and in solution; Dong *et al.* (1999) studied the solvent structure revealed by crystals grown in  $\mu$ g and in gel; Otalora *et al.*, (2001) studied the depletion zone in solution and in gel. In all these experiments the protein was dissolved in a gel medium. We propose a systematic comparison to understand the effect of each sub-environments (solution, gel, ground,  $\mu$ g): in our set up, both the protein and the precipitant are in gel, thus avoiding discontinuity in the transport mechanism, and making the comparative interpretation clearer. This complete comparison has so far never been described in the past.

### 1.2. System under study

Our system is not a globular protein. Indeed, it is a rod-like polypeptide with a repeating sequence (Pro-Pro-Gly)<sub>10</sub>, referred to as (PPG)<sub>10</sub>, which adopts a structural motif typical of collagen-like triple helix. (PPG)<sub>10</sub> is well characterized both from a thermodynamic (Holmgren *et al.*, 1999; Locardi *et al.*, 1999) and a crystallographic (Kramer *et al.*, 1998; Berisio *et al.*, 2000; Berisio *et al.*, 2002b) point of view. During the previous STS-95 space-

mission, (PPG)<sub>10</sub> crystals were grown in solution onboard the space-shuttle showing fewer crystals in the middle of the APCF reactors. Furthermore, a crystal motion was monitored, that was largely smaller than usually observed. In some reactors after about 200 hours, the growth was still incomplete (Carotenuto *et al.*, 2001), hence to analyse as many aspects as possible of the whole crystallisation process in  $\mu\text{g}$ , a longer time was requested, as provided by the International Space Station (ISS) mission. We planned our crystallization experiments of (PPG)<sub>10</sub> in  $\mu\text{g}$  with the twofold target: 1) to compare four different crystallization environments (solution on ground, gel on ground, solution in  $\mu\text{g}$  and gel in  $\mu\text{g}$ ), thus to factorise contributions due to each sub-environment; and 2) to compare crystallization onboard two  $\mu\text{g}$  platforms, ISS and space shuttle (Berisio *et al.*, 2000; Carotenuto *et al.*, 2001).

## 2. Materials and methods

### 2.1. Materials

(PPG)<sub>10</sub> was purchased from Peninsula Laboratory. Poly(ethylene glycol) 400 (PEG 400) was purchased from Sigma; acetic acid, sodium acetate and low gelling temperature (36 °C) agarose from Fluka. Reagents were used without extra purification. All solutions were prepared using double distilled water and were degassed with He before filling the reactors. We used a membrane Spectra/Por MWCO 6-8000.

### 2.2. Crystallization

All measurements described in this section and crystallization experiments on ground were performed in a room at 20 ( $\pm 1$ ) °C. The pre-flight search for optimal conditions suitable to the ISS mission is described in Berisio *et al.* (2002a). The optimised crystallization conditions are reported in Table 1; conditions were duplicated for test of reproducibility. Both one- and two-blocks reactors (Bosch *et al.*, 1992) were used. One-block reactors, called FID, can be used either in free interface diffusion or dialysis configuration, by inserting or not a membrane. On the other hand, two-blocks reactors, called DIA, can only operate in dialysis modality. Each reactor has an identity code. We had allocated eight (four one-block and four two-blocks) APCF reactors (four used on ground and four in  $\mu\text{g}$ ). Here we used all reactors in the dialysis configuration.

For each gravity level, two reactors were filled with solution and two with gel. (PPG)<sub>10</sub> was dissolved in aqueous solutions containing acetic acid (HAc) and PEG 400 (Table 1). The precipitant was sodium acetate. Both protein and precipitant chambers were filled with 0.2 % w/v gel and used for the experiments in agarose gel (Berisio, *et al.* 2002a). The diffusion of sodium acetate through the membrane produces a pH increase (from pH 3 to 5.3), which leads to crystallization. We performed solubility measurements *versus* PEG 400 concentration, in the pH range 4-9 at the constant ionic strength of 0.2 M (unpublished data). Under the used crystallization conditions (pH = 5.3, HAc 0.04 M, NaAc 0.20 M, PEG 400 10 % v/v and 20 °C), the solubility value is 0.56 mg/ml. Therefore we used an initial super-saturation value of 9 (evaluated as a ratio between initial protein concentration and solubility data). We underline that the solubility was determined in solution, not in gel: this value was however used for the analysis in solution and gel as well. Therefore a possible effect of super or under saturation due to the gel may affect the comparison.

Finally, we performed density measurements for all the protein solutions (1.02 g/ml) by a vibrating tube (Anton Paar, Model DMA5000), whereas the crystal density value of 1.31 g/ml was taken from the literature (Sakakibara *et al.*, 1972). Therefore the

high density difference drives the sedimentation phenomenon, and the gravity level tunes it.

**Table 1**

Crystallization conditions and crystal size in each reactor. All reactors were assembled in a dialysis configuration.

Code	environment	Reactor type	Agarose <sup>1,2,3</sup> (% w/v)	Average crystal size (mm)
607	Gel/1g	FID	0.2	0.18 $\pm$ 0.05
405 <sup>4</sup>	Sol/1g	FID	0.0	-
602	Gel/1g	DIA	0.2	0.14 $\pm$ 0.04
603	Sol/1g	DIA	0.0	0.17 $\pm$ 0.06
403	Gel/ $\mu\text{g}$	FID	0.2	0.14 $\pm$ 0.05
410	Sol/ $\mu\text{g}$	FID	0.0	0.22 $\pm$ 0.06
612	Gel/ $\mu\text{g}$	DIA	0.2	0.18 $\pm$ 0.02
616	Sol/ $\mu\text{g}$	DIA	0.0	0.13 $\pm$ 0.04

<sup>1</sup>In the protein chamber (PPG)<sub>10</sub>, PEG 400 and HAc concentrations are the same in all the reactors (5 mg/ml, 10 % v/v and 0.04 M respectively)

<sup>2</sup>In the precipitant chamber PEG 400 and NaAc concentrations are the same in all the reactors (10 % v/v and 0.23 M respectively)

<sup>3</sup>Agarose concentrations are equal in the two chambers

<sup>4</sup>Reactor 405 dried out.

### 2.3. Space Mission and APCF

The  $\mu\text{g}$  experimentation was performed by using APCF, provided by the European Space Agency (ESA). Characteristics of the APCF facility and its reactors are described elsewhere (Bosch *et al.*, 1992). The APCF was launched onboard the space shuttle Discovery, (STS-105 flight, on August 10<sup>th</sup>, 2001) and landed onboard the space shuttle Endeavour (STS-108 Flight, on December 17<sup>th</sup>, 2001). The docking to the International Space Station was on August 12<sup>th</sup>, 2001, and the APCF was put in the EXPRESS Rack No. 1 of the US Lab Destiny on August 13<sup>th</sup>. The reactors were activated (plug rotated by 90°) on August 13<sup>th</sup> and deactivated on November 30<sup>th</sup>.

### 2.4. Video observation

On ground, a CCD colour camera (Leica CCD 200, 176 pixel/mm) monitored a DIA two-block reactor containing gel, with a large field of view. The configuration of the microscope (Leica MZ 125) and the software for recording images were made *ad hoc* by Leica Microsystem. This software managed the recording, with a time lapse, both for image acquisition and motor focus (eight different focuses) and will be available in an outcoming version of the software Leica IM1000. A total of 160 x 8 TIFF images (8 focuses totally) were acquired in parallel to the 4 month space mission. On board, a black and white CCD camera monitored two DIA two-blocks reactors (one filled with gel and one with solution), recording BMP images. The size of the field of view was 3.74 mm x 4.78 mm  $\pm$  0.01. The position of the protein chamber was not exactly equidistant from the camera, as there is a tolerance when mounting the top part of the reactor onto the reactor main body. This unfortunately resulted in a shift of the protein chamber against the field of view of the camera. This shows that the protein chamber was not completely covered by the camera, with a loss of more than 20 % of the field. Furthermore, because of a power problem on ISS, the recording of data and images stopped after 115 images (per focus) or 944 hours elapsed time after the activation of the experiments. Fortunately, 40 days were enough to monitor a complete crystal growth, even though information about the crystal history was lost by this accident. The average temperature of the APCF was 20  $\pm$  0.4 °C; but a few short (from 2 to 54 min) power stops occasionally raised it up to 22 °C. During transportation the APCF was loaded in suitable boxes kept at 18  $\pm$  1 °C. On the basis of unpublished solubility data measured in our laboratory, crystallization experiments are not supposed to be significantly affected by this temperature variation.

### 3. Results

All reactors were filled with protein and other reagents (see Table 1) in the laboratory of Prof. Giegé in Strasbourg. The Mission took place from August to December 2001. During the whole experiment a video recording was performed both on ground (for the gel) and in  $\mu\text{g}$  (both for gel and solution). In all of the space reactors, crystals were obtained. All space reactors were photographed prior to launch and after landing at the Kennedy Space Center, afterward in Strasbourg and finally in our laboratory. From these latter photographs crystal average size was measured and is listed in Table 1. Crystals in gel showed wrinkled surfaces. Crystal quality was assessed by X-ray diffraction as reported elsewhere (Berisio *et al.*, 2002a): the maximum resolution for crystals grown in solution and for crystals grown in gel is 1.2 Å and 1.45 Å, respectively. Some ageing effects must be considered for (PPG)<sub>10</sub> crystals grown in agarose gel. Although the diffractive power of the crystals grown in gel is lower than in solution, the observed resolution limit of 1.45 Å is still quite high (both in  $\mu\text{g}$  and on ground).

#### 3.1. Nucleation

An analysis of the appearance time of the crystals as a function of the distance from the membrane and from the walls was made, in order to investigate possible effects of transportation of precipitant agent. Insights on the time sequence of the appearance of the crystals and their initial distribution were obtained, according to the sensibility of the CCD camera-microscope equipment that is around 5–10  $\mu\text{m}$ .

In case of diffusive transport of the precipitant agent, if the homogenization time is longer than the nucleation time, the occurrence of a nucleation front that spreads through the chamber, once the reactor is activated, could be expected. Such a supersaturation gradient should give rise to a time distribution of crystals correlated to the distance from the membrane (Otalora & Garcia-Ruiz, 1997; Garcia-Ruiz *et al.* 2001b). Conversely, the absence of a relationship between the time of appearance of a given crystal and its distance from the membrane, along with an even time distribution of the crystals inside the chamber, were observed in all the three monitored reactors (code 602, 612 and 616 corresponding to gel on ground and in  $\mu\text{g}$ , solution in  $\mu\text{g}$  respectively). This trend seems to indicate that the appearance times (hence induction times) of (PPG)<sub>10</sub> crystals, under the used experimental conditions, are longer than the homogenization ones, both in  $\mu\text{g}$  and on ground. Therefore, nucleation occurs practically as in batch conditions, as already observed for FID and DIA APCF reactors (Garcia-Ruiz *et al.* 2001b). In gel, crystals appear almost uniformly inside the chamber for the duration of the mission. Also in solution, nucleation occurs uniformly into the whole protein chamber, but later crystals move towards the reactor walls, like described below.

Furthermore, the induction times are almost the same, (around 100 hours), in the three monitored environments, indicating no significant difference in nucleation rates.

#### 3.2. Morphology

The morphology observed by video of crystals grown in solution and gel, both in  $\mu\text{g}$  and on ground, was slightly different. The thickness and length have comparable sizes in gel (with a proportion of 1:2), whereas they are much more different (1:4) in solution. The observed morphology was better for crystals grown in one-block reactors (Bosch *et al.* 1992), indicating somewhat influence of the reactor geometry.

#### 3.3. Crystal distribution

The spatial distribution has been analysed for the free-floating crystals, because no focus plane was set on the walls: on the images,

the protein chamber was uniformly divided into 64 cells, analogously to a previous analysis (Carotenuto *et al.*, 2001). The distribution of crystals grown in solution in  $\mu\text{g}$  shows that  $85 \pm 10\%$  of crystals are close to the reactor walls (plane yz in Fig. 1) even though not all of them are stuck. These data are very consistent with the STS-95 results (Carotenuto *et al.*, 2001), showing that the two space platforms (Space Shuttle and ISS) provide reproducible results about crystal distribution in solution. From the time evolution of the crystal distribution, it is apparent that crystals first nucleated in the middle focal plane and then migrate towards the yz wall. Therefore, the final distribution in solution is not due to a heterogeneous nucleation, but to the crystal motion itself. The percentage of floating crystals in gel is higher ( $50 \pm 15$  and  $75 \pm 8\%$  on ground and in  $\mu\text{g}$  respectively) than in solution (0 and  $15 \pm 10\%$  on ground and in  $\mu\text{g}$  respectively). In the STS-95 mission no experiment in gel is available for comparison.

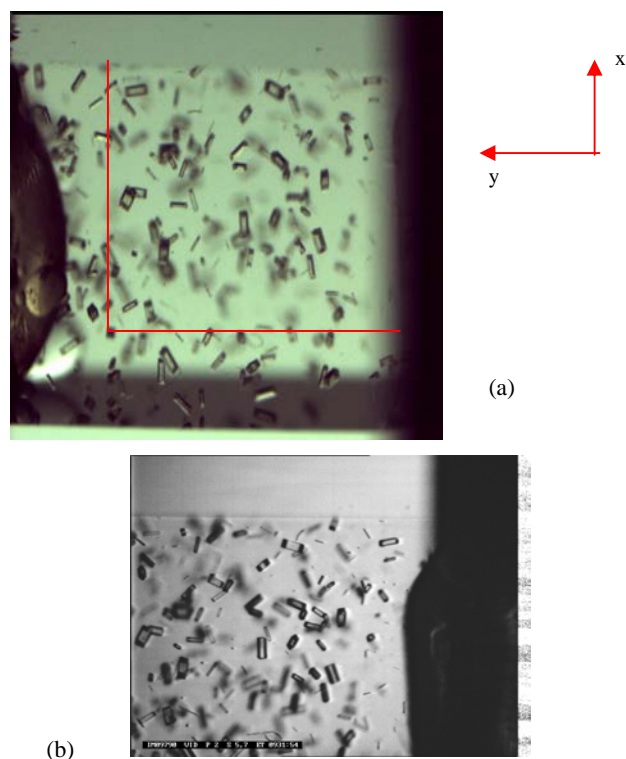


Figure 1

Images of the APCF reactor used in  $\mu\text{g}$  with gel (code 612): (a) whole image recorded after landing in our laboratory. The internal frame refers to the part recorded on ISS. (b) The last image recorded onboard the ISS. The xy reference frame is also reported.

#### 3.4. Crystal motion

No motion was observed in gel. In fact, the pore size at 0.2% agarose concentration (Pernodet *et al.*, 1997) and ionic strength 0.17 M (Maaloum *et al.*, 1998) is around 3  $\mu\text{m}$ , and no sedimentation or motion can be expected under these conditions (García-Ruiz *et al.*, 2001a). Therefore, we report only the analysis of crystal motions in solution.

On board the ISS, we have observed motion of only some crystals, whereas others do not move. In Fig. 2, the coherent displacement of five selected crystals along the preferential direction is reported; the displacement along other directions is negligible. All crystals that reach the wall surface stay stuck on that, thus irreversibly affecting the final crystal distribution. The ultimate

effect is that crystals growing in the bulk of the solution move coherently towards a wall, justifying the difference between the initial nucleation distribution and the final crystal distribution inside the reactor. During the previous space-shuttle mission (Carotenuto *et al.*, 2001) a very limited incoherent motion of a few (PPG)<sub>10</sub> crystals was observed. The mostly coherent and parallel movement of the crystals has been observed for the first time. It can be linked to the presence of accelerations on large scale, like residual acceleration or g-jitters on the ISS. The average velocity is comparable in the two platforms (around 1  $\mu\text{m h}^{-1}$ ); considering the Stokes regime, this velocity is compatible with a residual acceleration of the order of 1  $\mu\text{g}$ . The correlation with acceleration data collected onboard the ISS is in progress.

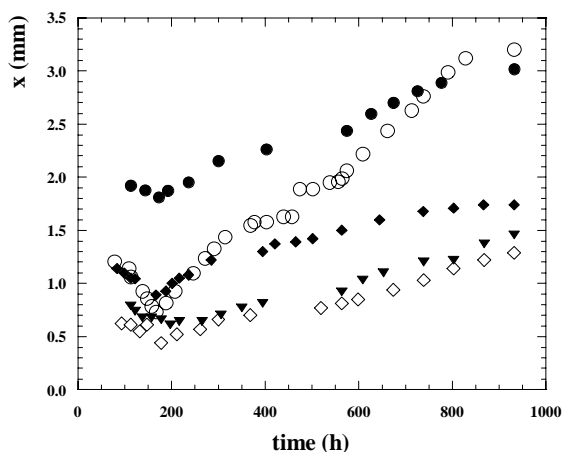


Figure 2

Displacement along the x direction (defined in Fig. 1) of five crystals observed in the reactor code 616 (solution in  $\mu\text{g}$ ) onboard the ISS. Symbols refer to different crystals.

### 3.5. Crystal growth rate

The linear growth rate of the crystals has been measured in all of the three reactors under observation (codes 602, 612 and 616 corresponding to experiments with gel on ground and in  $\mu\text{g}$ , and solution in  $\mu\text{g}$  respectively). Both the thickness and length of the crystals were measured. For solution grown crystals, we chose to measure the growth rate for still crystals with no change of orientation along with the time.

In Fig. 3 we report the time evolution of the crystal length for the three monitored environments. A common trend is shown in all the monitored environments: 1) an initial induction time of 90-100 hours to reach the supersaturation necessary for the nucleation steps; 2) appearance of the crystal and steep increase of the crystal size; 3) cessation of the growth after about 200-400 hours, depending on the final crystal size. The analysis does not indicate any dependence of the growth rate on the position of the crystal inside the reactor.

The analysis of data in Fig. 3 showed the growth rate to be the same in all of the three monitored environments ( $6.4 \pm 0.7 \text{ \AA s}^{-1}$ ). The parallel use of solution and gel or solution on ground and solution in  $\mu\text{g}$  can provide useful information about the mechanism of crystal growth. In fact, assuming the only difference between two crystallization environments is their transport properties and not the crystallization mechanism or the solubility value, then a comparative analysis allows distinguishing if growth is controlled by diffusion or by interface kinetics. In the case of (PPG)<sub>10</sub>, under the used experimental conditions, the growth rate seems to be controlled by kinetics at the interface, as found in the case of the Asp-tRNA synthetase (Zhu *et al.*, 2001).

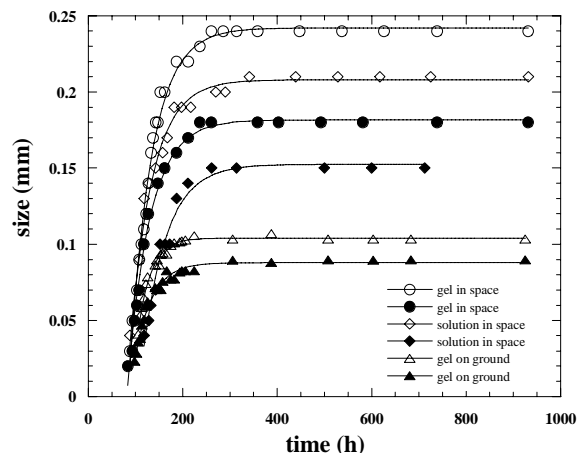


Figure 3

Examples of crystal length vs time for the three monitored environments.

### 4. Conclusion

For the first time it was possible to obtain a comparison of the (PPG)<sub>10</sub> crystal growth between two platforms available for experimentation in  $\mu\text{g}$  (space shuttle and ISS) and among four crystallization environments (solution on ground and in  $\mu\text{g}$ , gel on ground and  $\mu\text{g}$ ). It is auspicious that the same comparison will be performed for other proteins, so that the behaviour can be confirmed as general or just peculiar of one isolated system.

The crystal growth experimentation in the long space mission onboard the ISS (flights STS 105 and STS108) allowed to reach the complete growth, differently from the previous STS-95 onboard the space shuttle (105 and 8 days of active phase respectively). Because of technical problems onboard the ISS, the image analysis is available only for the first 40 days out of 4 months, covering less than 80 % of the whole reactor. As expected, ISS resulted a  $\mu\text{g}$  platform different from space shuttle. As crystal motions are still observed but they are more coherent and parallel, with essentially the same average speed, relevant steady accelerations are supposed to take place onboard the ISS. Consequently the final distribution in solution is strongly affected by this motion. The crystal appearance time and the growth rate are comparable in all the crystallization environments. These observations suggest that the crystal growth mechanism for (PPG)<sub>10</sub> is kinetically controlled, under the used experimental conditions. The crystal growth of this long polypeptide has been well characterised from many physical chemistry points of view, making (PPG)<sub>10</sub> a model for crystallogenic study of non globular proteins.

The authors would like to thank Drs. Vitagliano and Berisio from CNR of Naples for useful discussion; Drs. Giegé and Lorber from CNRS of Strasbourg for hosting during the filling session and for providing picture of reactors after landing; Drs. Minster and Di Palermo from ESA; Drs. Potthast, Stapelmann and Lautenschlager from ASTRUM and Dr. Parlatano from Leica-Microsystem. ASI (Italian Space Agency) is acknowledged for the financial support.

### References

- Amsden, B. (1998). *Macromolecules*, **31**, 8382-8395.
- Berisio, R., Vitagliano, L., Sorrentino, G., Carotenuto, L., Piccolo, C., Mazzarella, L. & Zagari, A. (2000). *Acta Cryst.* **D56**, 55-61.

- Berisio, R., Vergara, A., Vitagliano, L., Sorrentino, G., Mazzarella, L. & Zagari A. (2002a). *Acta Cryst. D58*, 1695-1699.
- Berisio, R., Vitagliano, L., Mazzarella, L. & Zagari, A. (2002b). *Protein Sci.* **11**, 262-270.
- Bosch, R., Lautenschlager, P., Potthast, L. & Stapelmann, J. (1992). *J. Cryst. Growth*, **122**, 310-316.
- Carotenuto, L., Berisio, R., Piccolo, C., Vitagliano, L. & Zagari, A. (2001). *J. Cryst. Growth*, **232**, 481-488.
- Chayen, N. E., Snell, E. H., Helliwell, J. R. & Zagalsky, P. F. (1997). *J. Cryst. Growth*, **171**, 219-225.
- Chayen, N. E. & Helliwell, J. R. (1999). *Nature (London)*, **398**, 20-20.
- Couzin, J. (1998). *Science*, **281**, 497-498.
- DeLucas, L. J., Long, M. M., Moore, K. M., Rosenblum, W. M., Bray, T. L., Smith, C., Carson, M., Narayana, S. V. L., Carter, D., Clark, A. D. Jr., Nanni, R. G., Ding, J., Jacobo-Molina, A., Kamer, G., Hughes, S. H., Arnold, E., Einspahr, E., Clancy, L. L., Rao, G. J., Cook, P. F., Harris, B. G., Munson, S. H., Finzel, B. C., McPherson, A., Weber, P. C., Lowandowski, F., Nagabhushan, T. L., Trotta, P. P., Reichert, P., Navia, M. A., Wilson, K. P., Thomson, J. A., Richards, R. R., Bowersox, K. D., Mead, C., Baker, E. S., Bishop, S. P., Dunbar, B. J. & Trinh, E. (1994). *J. Cryst. Growth*, **135**, 183-195.
- DeLucas, L. J. (2001). *DDT*, **6**, 734-744.
- Dong, J., Boggon, T. J., Chayen, N. E., Raftery, J., Bi, R.-C. & Helliwell, J. R. (1999). *Acta Cryst. D55*, 745-752.
- García-Ruiz, G. M., Gavira, J. A., Otalora, F., Guasch, A. & Coll, M. (1993). *Mat. Res. Bull.* **28**, 541-546.
- García-Ruiz, J.M. & Otalora, F. (1997). *J. Cryst. Growth*, **182**, 155-167.
- García-Ruiz, J. M., Novella, M. L., Moreno, R. & Gavira, J. A. (2001a). *J. Cryst. Growth*, **232**, 165-172.
- García-Ruiz, J. M., Drenth, J., Riés-Kautt, M., Tardieu, A. (2001b). *A world without gravity – research in space for health and industrial processes* edited by G. Seibert, pp. 159-171, ESA SP.
- Giegé, R. & McPherson, A. (2001). *International Tables For Crystallography*, Vol. F, Appendix 4, 81-99.
- Henisch, H. K. (1988). *Crystal growth in gels and Leisegang Rings*. New York: Cambridge University Press.
- Holmgren, S. K., Bretscher, L. E., Taylor, K. M. & Raines, R. T. (1999). *Chem. Biol.* **6**, 63-70.
- Johnson, E. M., Berk, D. A., Jain, R. K. & Deen, W. M. (1996). *Biophys. J.* **70**, 1017-1026.
- Kong, D. D., Kosar, T. F., Dungan, S. R. & Phillips, R. J. (1997). *AIChE J.* **43**, 25-32.
- Kouwijzer, M. & Pérez, S. (1998). *Biopolymers*, **46**, 11-29.
- Kramer, R. Z., Vitagliano, L., Bella, J., Berisio, R., Mazzarella, L., Brodsky, B., Zagari, A. & Berman, H. M. (1998). *J. Mol. Biol.* **280**, 623-638.
- Locardi, E., Kwak, J., Scheraga, H. A. & Goodman, M. (1999). *J. Phys. Chem. B*, **103**, 10561-10566.
- Lorber, B., Sauter, C., Robert, M.-C., Capelle, B. & Giegé, R. (1999). *Acta Cryst. D55*, 1491-1494.
- Maaloum, M., Pernodet, N. & Tinland, B. (1998). *Electrophoresis*, **19**, 1606-1610.
- McPherson, A. (1996). *Crystallogr. Rev.* **6**, 157-307.
- Miller, T. Y., He, X. & Carter, D. C. (1992). *J. Cryst. Growth*, **122**, 306-309.
- Muhr, A. H. & Blanshard, J. M. (1982). *Polymer*, **23**, 1012-1026.
- Normand, V., Lootens, D. L., Amici, E., Plucknett K. P. & Aymard P. (2000). *Biomacromolecules*, **1**, 730-738.
- Otalora, F & García -Ruiz, J. M. (1997). *J. Cryst. Growth*, **182**, 141-154.
- Otalora, F., Novella, M. L., Gavira, J. A., Thomas, B. R. & García -Ruiz, J. M. (2001). *Acta Cryst. D57*, 412-417.
- Pernodet, N., Maaloum, M. & Tinland, B. (1997). *Electrophoresis*, **18**, 55-58.
- Robert, M. C. & Lefauchaux, F. (1988). *J. Cryst. Growth*, **90**, 358-367.
- Sakakibara, S., Kishida, Y., Okuyama, K., Tanaka, N., Ashida, T. & Kakudo, M. (1972). *J. Mol. Biol.* **65**, 371-373.
- Snell, E. H., Boggon, T. J., Helliwell, J.R., Mosowitz, M. E. & Nadarajah, A. (1997). *Acta Cryst. D53*, 747-755.
- Stigter, D. (2000). *Macromolecules*, **33**, 8878-8889.
- Zhu, D.-W., Lorber, B., Sauter, C., Ng, J. D., Bénas, P., Le Grimemec, C. & Giegé, R. (2001). *Acta Cryst. D57*, 552-558.